

Bright, multicoloured light-emitting diodes based on quantum dots

QINGJIANG SUN¹, Y. ANDREW WANG^{2*}, LIN SONG LI², DAOYUAN WANG², TING ZHU³, JIAN XU³, CHUNHE YANG¹ AND YONGFANG LI^{1*}

¹Beijing National Laboratory for Molecular Sciences, CAS Key Laboratory of Organic Solids, Institute of Chemistry, Chinese Academy of Sciences, Beijing 100080, China

²Ocean NanoTech, 700 Research Center Boulevard, Fayetteville, Arkansas 72701, USA

³Department of Engineering Science and Mechanics, Penn State University, University Park, Pennsylvania 16802, USA

*e-mail: liyf@iccas.ac.cn; awang@oceannanotech.com

Published online: 18 November 2007; doi:10.1038/nphoton.2007.226

Quantum-dot-based LEDs are characterized by pure and saturated emission colours with narrow bandwidth, and their emission wavelength is easily tuned by changing the size of the quantum dots. However, the brightness, efficiency and lifetime of LEDs need to be improved to meet the requirements of commercialization in the near future. Here, we report red, orange, yellow and green LEDs with maximum luminance values of 9,064, 3,200, 4,470 and 3,700 cd m^{-2} , respectively, the highest values reported so far. Solution-processable core-shell quantum dots with a CdSe core and a ZnS or CdS/ZnS shell were used as emissive layers in the devices. By optimizing the thicknesses of the constituent layers of the devices, we were able to develop quantum-dot-based LEDs with improved electroluminescent efficiency (1.1–2.8 cd A^{-1}), low turn-on voltages (3–4 V) and long operation lifetimes. These findings suggest that such quantum-dot-based LEDs will be promising for use in flat-panel displays.

In recent years, the development of low-cost, solution-based synthesis of colloidal semiconductor nanocrystals or quantum dots (QDs) has stimulated studies on QD-based LEDs (QD-LEDs), which exhibit pure and saturated colours with a narrow bandwidth (full-width at half-maximum (FWHM) of the electroluminescence (EL) peak of $\sim 30 \text{ nm}$)^{1–16}. Emission from the QD-LEDs can easily be tuned by varying the size or the composition of the QDs without changing their processing properties. One device fabrication procedure can therefore be used for different QDs to produce emissions over a broad wavelength range, covering the visible^{1–13} and near-infrared^{14–16} regions. In addition, high fluorescence quantum yield (QY) and photochemical stability can be achieved by careful modification of the nanocrystal surface, which may favour an improvement in efficiency and stability of the devices^{17,18}. These unique properties make QD-LEDs promising candidates for applications in flat-panel displays (FPDs)¹⁹ and lighting^{20,21}.

Until now, almost all the best performances of QD-LEDs have been achieved on devices having just one monolayer (ML) of QDs, because thicker QD layers in QD-LEDs give rise to higher operating voltages and lower carrier-injection efficiencies as a result of slow dot-dot transport^{3,4,6–9,12,15}. A device with a CdSe/ZnS core-shell QD ML between a hole-transport layer (HTL) of *N,N'*-diphenyl-*N,N'*-bis-*m*-tolylbenzidine and an electron-transport layer (ETL) of tris(8-hydroxyquinoline) aluminium (Alq_3) has been demonstrated, which resulted in a red-emitting QD-LED with a maximum EL external quantum efficiency (EQE) of $>2\%$ at peak wavelength³. Maximum luminance values of 2,000 cd m^{-2} , and later 7,000 cd m^{-2} , have been recorded, although a large fraction of the emission comes from the blue- or red-emitting organic cladding layers^{3,6}. Red-emitting QD-LEDs

were recently fabricated with a ML of CdSe/CdS core-shell QDs and a thermally polymerized HTL (ref. 4). The QD-LEDs exhibited a narrower (30 nm, FWHM) EL bandwidth, an EQE of 0.8% at 100 cd m^{-2} , and a maximum brightness greater than 1,000 cd m^{-2} . $\text{Cd}_x\text{Zn}_{1-x}\text{Se}/\text{Cd}_y\text{Zn}_{1-y}\text{S}$ ML core-shell QDs have been incorporated into a four-layered structure, and colour-saturated green emission was achieved with an EQE of 0.81% at 140 cd m^{-2} (ref. 8). QD-LEDs have also been fabricated by incorporating QDs into a polymer matrix or spin-coating QD films from concentrated solutions, but all the devices exhibited low EQEs ($<0.2\%$), high turn-on voltage ($>6 \text{ V}$), low maximum luminance ($<600 \text{ cd m}^{-2}$) and moderate lifetimes ($t_{80\%} = 200 \text{ h}$ at 10 cd m^{-2} ; $t_{50\%} = 40 \text{ h}$ at $\sim 120 \text{ cd m}^{-2}$)^{1,2,7,13,21}.

Although QD-LEDs with ML QDs have the advantages of higher efficiency and lower turn-on voltages, their output power, maximum luminance and colour purity are limited owing to the low chromophore quantity and the poor confinement of excitons in the active QD region. We report high-performance red, orange, yellow and green QD-LEDs based on QDs with a CdSe core and a ZnS or CdS/ZnS shell. Their maximum luminance reached 9,064, 3,200, 4,470 and 3,700 cd m^{-2} , respectively, the highest values reported so far for correspondingly coloured QD-LEDs. Moreover, the QD-LEDs had low turn-on voltages (3–4 V), improved efficiency (1.1–2.8 cd A^{-1}), saturated colour (narrow EL bandwidth) and a longer operation time at an higher luminance ($t_{50\%} = 300 \text{ h}$ at $>1,100 \text{ cd m}^{-2}$). Uniform and defect-free EL emission from the QDs over a surface area of $1.5 \text{ cm} \times 2.5 \text{ cm}$ was realized, suggesting promise in the application of the QD-LEDs in future large-area FPDs. The superior performance of the QD-LEDs arises from the careful preparation of highly purified, uniform and monodispersed

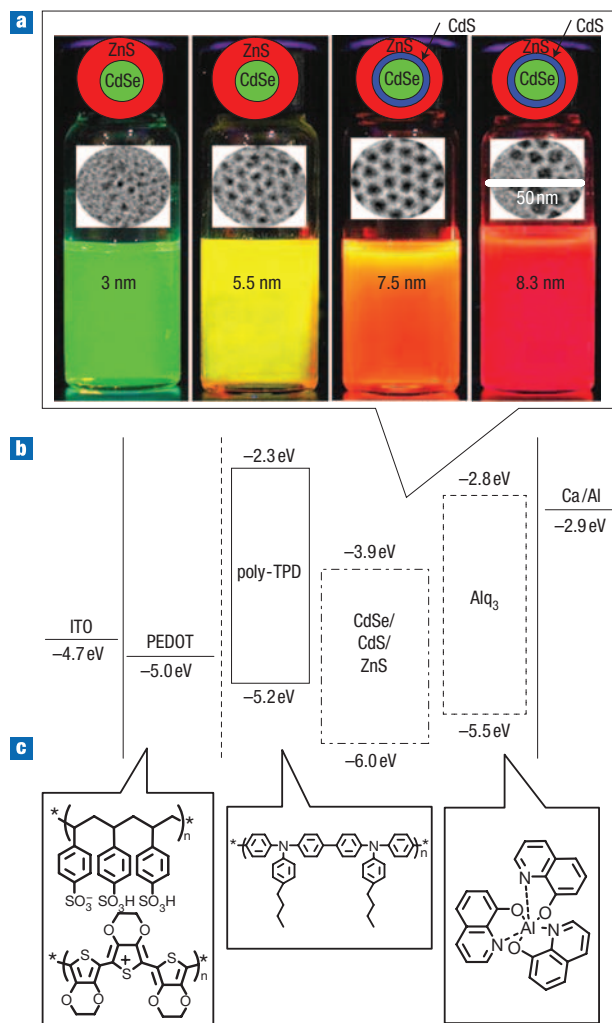


Figure 1 Structures, images and HOMO and LUMO energy levels of the QD-LEDs. **a**, Core-shell structures (top), transmission electron microscopy (TEM) images of the QDs (middle), and PL photographs of the four-coloured QD solutions in toluene (bottom) for the QD-LEDs. The values 3 nm, 5.5 nm, 7.5 nm and 8.3 nm indicate the size of the QDs. **b**, HOMO and LUMO energy levels of the materials involved in the QD-LED. The HOMO and LUMO values for poly-TPD and Alq₃ were obtained from refs 26–28. The HOMO of the red QD was determined by electrochemical cyclic voltammetry (see the Supplementary Information). The LUMO of the red QD was estimated from its bandgap and the HOMO level. **c**, Molecular structures of PEDOT, poly-TPD and Alq₃.

colloidal core-shell QDs, and optimization of the thicknesses of the polymer HTL, the QD layer and the ETL.

RESULTS AND DISCUSSION

PREPARATION OF HIGH-QUALITY QDs

The red, orange, yellow and green semiconductor QDs used in this work all had core-shell structures with the same CdSe core and a ZnS or CdS/ZnS shell. The ZnS or CdS/ZnS shell increases the photostability of the QDs, because the energy levels of CdS/ZnS or ZnS shells are high enough to confine the holes to the CdSe core while electrons are delocalized throughout the structure, making the nanocrystal highly photo-oxidatively stable⁷. The emission colour was tuned by manipulating the size of the CdSe

core and controlling the shell structures with either a ZnS single shell or CdS/ZnS double shell. High-quality QDs with high photoluminescence QY (PL-QY), narrow size distribution, narrow emission bandwidth and high purity were prepared with the low-toxic chemical method as reported in the literature^{22,23}. For use in the QD-LEDs, all the as-prepared QDs were subjected to further purification by repeating multistep purification processes for removing organic ligands. After purification, the red, orange and yellow QDs were in solid powder form with QY higher than 30% in toluene, whereas the green QDs were still in liquid solution, with a QY of ~10% in toluene, owing to their smaller size. During the purification process, the removal of organic ligands from the QDs produces surface defects that may trap charges. The green QDs, with their smaller size (3 nm, as shown in Fig. 1a), will have a larger surface area and more surface defects, thus their fluorescent QY is greatly reduced. The structures and optical properties of the QDs are listed in Table 1. The PL emission peaks of the red, orange, yellow and green QD toluene solutions are located at 610 nm, 589 nm, 567 nm and 517 nm, respectively, with an FWHM range of 21–28 nm. Figure 1a shows the core-shell structures and transmission electron microscopy (TEM) images of the QDs, as well as PL photographs of the four-coloured QD solutions in toluene.

Different synthetic strategies were used to control the emission wavelength of the CdSe core and obtain high PL-QY CdSe/ZnS core-shell QDs. First, small-sized (2 nm in diameter) CdSe core QDs with a PL peak located at 500 nm for obtaining green core-shell QDs were synthesized by choosing Cd-octadecylphosphonic acid (ODPA) as cadmium precursor. Meanwhile, the CdSe core QDs for yellow, orange and red core-shell QDs with PL peaks at approximately 560 nm, 570 nm and 580 nm, respectively, were prepared using cadmium stearate^{22–24}. ZnS was used as the outer shell for its ease of surface purification and its high stability. A ZnS single shell was used for yellow and green emission QDs, whereas a CdS/ZnS double shell was designed to obtain orange and red emission QDs, because the overlap of the electron work functions between CdSe and CdS causes the emissions of CdSe/CdS/ZnS core-shell QDs to be redshifted (more than 40 nm redshift in our experiments) compared with that of the CdSe/ZnS core-shell QDs.

STRUCTURAL DESIGN OF THE QD-LED DEVICES

The trilayer structure of indium tin-oxide (ITO)/poly(ethylenedioxythiophene):polystyrene sulphonate (PEDOT:PSS) (25 nm)/HTL (45 nm)/QDs (~15–20 nm)/ETL (35 nm)/Ca (15 nm)/Al (150 nm) was used in the fabrication of the QD-LEDs, with ITO/PEDOT:PSS as the anode, poly(*N,N'*-bis(4-butylphenyl)-*N,N'*-bis(phenyl)benzidine) (poly-TPD) spin-coated from its chlorobenzene solution as HTL, QD layers spin-coated from their toluene solutions as emissive layers, Alq₃ as ETL, and Ca/Al as the cathode (Fig. 1b).

The molecular structures and energy levels of the materials involved in a red-emitting QD-LED are shown in Fig. 1b,c. PEDOT:PSS was used as the buffer layer on the anode mainly to increase the anode work function from 4.7 eV (ITO) to 5.0 eV and to reduce the surface roughness of the anode to obtain stable and pin-hole-free electrical conduction across the device²⁵. Poly-TPD was used as the HTL in consideration of the fact that its highest occupied molecular orbital (HOMO) level is 5.2 eV, which is very close to the work function of the ITO/PEDOT:PSS anode, and also because it possesses an excellent hole-transport capability²⁶. Moreover, poly-TPD has proven to be a good resistor to nonpolar organic solvents such as toluene and xylene²⁷. In contrast with the use of thermally polymerized polymer HTLs (ref. 4), with which the underlying PEDOT:PSS

Table 1 Structural and optical characteristics of four-coloured QD solutions in toluene.

	Green QDs	Yellow QDs	Orange QDs	Red QDs
Core-shell structure	CdSe/ZnS	CdSe/ZnS	CdSe/CdS/ZnS	CdSe/CdS/ZnS
Absorption (nm)	506	546	577	600
PL (nm)	517	567	589	610
FWHM (nm)	25	28	22	21
QY: as-prepared*	>70%	>70%	>70%	>70%
QY purified for QD-LED*	10%	30%	40%	35%

*QY values of the QDs were measured in toluene solutions.

buffer layer could be destroyed through thermal crosslinking at the high temperatures required for annealing, because the poly-TPD layer does not need a high annealing temperature, the PEDOT:PSS buffer layer can be used. Alq₃ was chosen as the ETL because of its good electron-transport capability²⁸ and its interfacial phase compatibility with the QD layer⁶.

EL PERFORMANCE OF THE QD-LEDs

Figure 2a shows typical current and luminance curves as a function of applied voltage for the four-coloured QD-LEDs. The variation profile of EL efficiencies, including luminous efficiency and power efficiency of the four-coloured devices across the entire measured luminance range, is shown in Fig. 2b. All the devices demonstrated low turn-on voltages of 3–4 V, confirming the minimized barrier height for charge injection into the QD-LEDs. The maximum luminance and luminous efficiency values respectively reached 9,064 cd m⁻² and 2.8 cd A⁻¹ for the red device, 3,200 cd m⁻² and 1.8 cd A⁻¹ for the orange device, 4,470 cd m⁻² and 1.3 cd A⁻¹ for the yellow device, and 3,700 cd m⁻² and 1.1 cd A⁻¹ for the green device. The maximum luminances are the highest values reported so far for correspondingly coloured QD-LEDs. At standard display brightness (100–500 cd m⁻²), the four-coloured QD-LEDs all showed relatively stable and high luminous efficiencies of 2.68, 1.46, 1.30 and 1.06 cd A⁻¹ at 100 cd m⁻², changing to 2.64, 1.14, 1.12 and 1.06 cd A⁻¹ at 500 cd m⁻², for the red-, orange-, yellow- and green-emitting devices, respectively. The power efficiencies of the four-coloured QD-LEDs consistently reached their maxima at near turn-on and then decreased to 0.33–1.11 lm W⁻¹ (green to red) at 100 cd m⁻² and to 0.27–0.78 lm W⁻¹ at 500 cd m⁻².

The EL spectra of the four-coloured QD-LEDs, operating at different luminances (voltages), are shown in Fig. 2c; images of the QD-LEDs under operation are presented in the insets of the figure. Among the photographs, the red-emitting QD-LED exhibited bright, uniform and defect-free EL emission over a surface area of 1.5 cm × 2.5 cm, which is the largest area reported so far^{6,19}, indicating promise for the application of QD-LEDs in large-area FPDs. The EL emission peaked at 619 nm, 595 nm, 576 nm and 525 nm for the red-, orange-, yellow- and green-emitting devices, respectively. The FWHMs of the EL peaks are 28 nm for the red and orange QD-LEDs, 35 nm for the yellow, and 32 nm for the green devices, demonstrating the colour-saturated light emission of the QD-LEDs. Furthermore, the EL spectra of all the QD-LEDs remained stable within the whole measured luminance (voltage) range, from ~10 cd m⁻² to the maximum luminance. There is no obvious contribution from the polymer HTL or organic ETL in the EL spectra of the QD-LEDs. The Commission Internationale de l'Éclairage (CIE) coordinates of the emitted lights of the QD-LEDs are (0.653, 0.324), (0.544, 0.418), (0.480, 0.485) and (0.202, 0.676) for red-,

orange-, yellow- and green-emitting devices, respectively. When the CIE coordinates of the QD-LEDs are compared with the colour triangle of the National Television System Committee (NTSC), as shown in Fig. 2d, all four QD-LED colours are in excess of the high-definition-television (HDTV) standard^{6,8,19}.

A lifetime test of the red-emitting QD-LED was performed by operating the device under vacuum at a constant bias of 13 V and measuring the luminance variation as a function of time, as shown in Fig. 3. The red-emitting QD-LED was stable over hundreds of hours of continuous operation at a brightness of >1,100 cd m⁻², with a slow decay to 50% of its initial value after 300 h.

OPTIMIZATION OF THE THICKNESS OF THE QD LAYER

In optimizing the device structure of the QD-LEDs, it was found that the thickness of the QD layer played a critical role in colour purity, EL efficiency and maximum luminance of the devices. Figure 4a shows EL efficiency as a function of the injection current for the red-emitting QD-LEDs with QD layer thicknesses of 2, 3 and 4 MLs. Clearly, the EL efficiency of the device with a QD layer thickness of 2 MLs was higher than that of the devices with QD layers of 3 or 4 MLs thickness in the whole injection current range, indicating that a thicker QD layer limited the EL efficiency of the red-emitting QD-LEDs, owing to the poorer charge transportation between QDs.

Thinner emissive layers down to monolayer QDs, however, had increased leakage current through the QD layer without radiative recombination owing to the presence of voids, grain boundaries and interstitial spaces in the QD monolayers. This is apparent in the EL spectra of the QD-LEDs having different QD layer thicknesses, as shown in Fig. 4b. When the thickness of the QD layer is less than 2 MLs, the emission from Alq₃ appears in the spectra characterized by the maxima at 540 nm, leading to deterioration of the colour purity of the QD-LEDs. The Alq₃ contribution to the EL signal originates from the leakage of holes into the ETL in the QD-LEDs (ref. 3). Incorporating a 10-nm hole-blocking layer of 2,9-dimethyl-4,7-diphenyl-1,10-phenanthroline (BCP) between the QD layer and the ETL, the Alq₃ emission still appeared at high operating voltages, and the QD-LEDs showed lower efficiency owing to the poorer electron-transport capability of BCP when compared with Alq₃. By combining the results in Fig. 4a and b, we determined 2 MLs to be the optimal thickness for the QD layer of the red-emitting QD-LEDs.

The optimal thickness of the QD layer in different coloured QD-LEDs is dependent on the size and structure of the QDs. The inset of Fig. 4b shows the variation of the EL spectra of the green-emitting QD-LEDs with different QD layer thicknesses. The optimal thickness in the green device is ~7 MLs, which differs greatly from that of the red device. The best device performance was demonstrated for the orange- and yellow-emitting QD-LEDs with layer thicknesses of ~2.5 MLs and ~4 MLs,

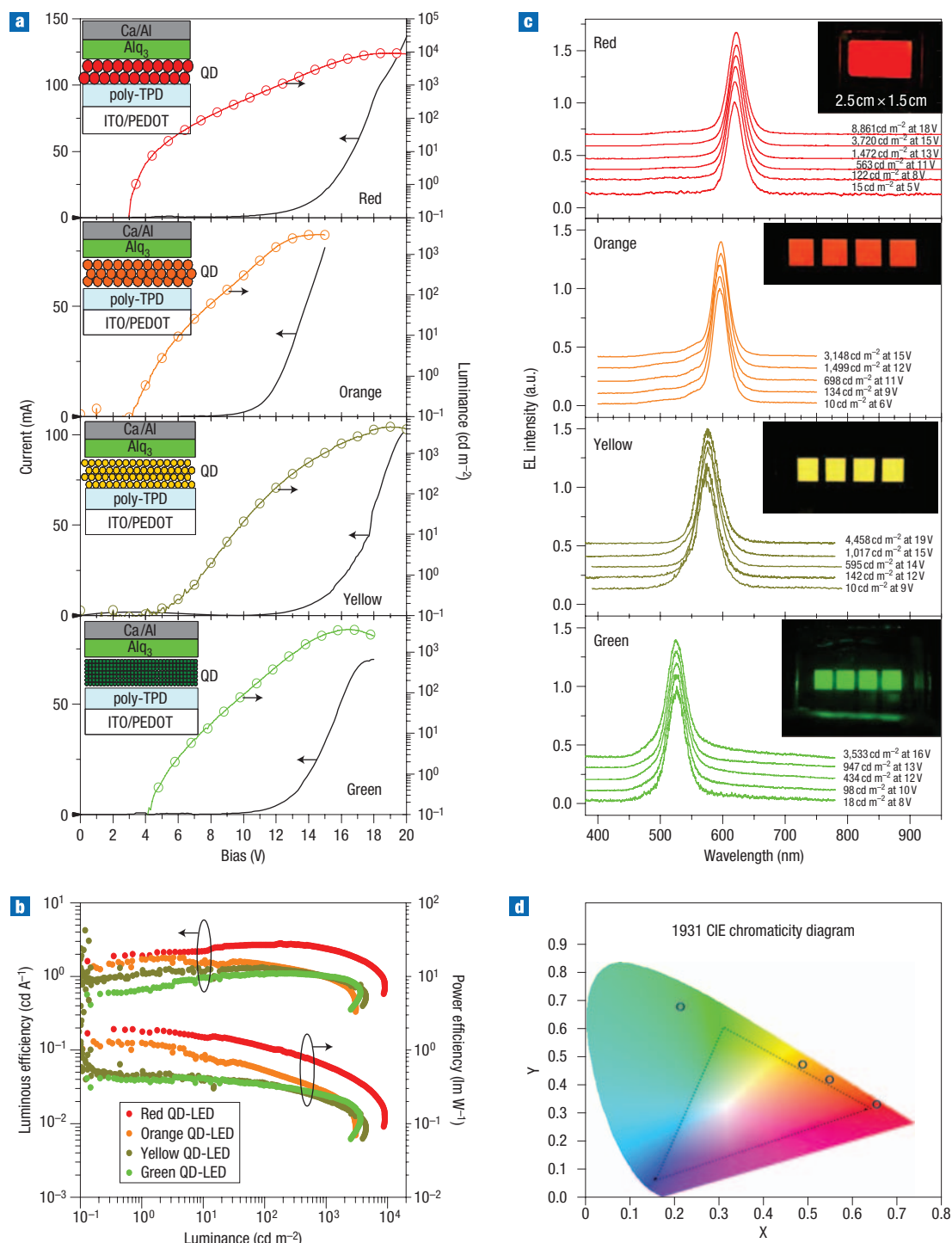


Figure 2 Electroluminescence performance of the QD-LEDs. **a**, Current/voltage and luminance/voltage characteristics of red-, orange-, yellow- and green-emitting QD-LEDs. The insets show schematic device configurations of the corresponding QD-LEDs. **b**, Luminous efficiency and power efficiency of the QD-LEDs as a function of luminance. The arrow pointing left indicates that the curves relate to luminous efficiency. **a, b** The arrows pointing to the right indicate curves that relate to right axis and arrows pointing to the left indicate curves that relate to the left axis. **c**, EL spectra of the red-, orange-, yellow- and green-emitting QD-LEDs operating at different luminances (voltages). The insets show images of the devices under operation. **d**, CIE coordinates of the emitted lights of the four-coloured QD-LEDs with respect to the colour triangle of NTSC.

respectively. The variation of the optimal layer thickness with the size and shell structure of the QDs is consistent with the reported results, which suggest that free-carrier injection into smaller QDs exhibits considerably lower efficiency than injection into larger QDs with

the same composition owing to the increased mismatch between the HOMOs of the QDs and underlying HTLs (refs 3, 6, 8, 9). This observation is of profound significance and provided the essential guidance in the device design of our QD-LEDs.

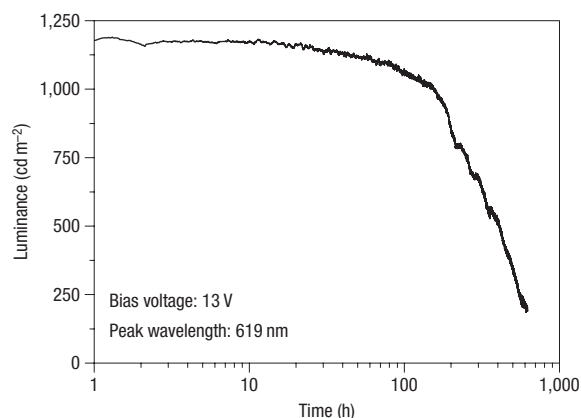


Figure 3 Lifetime characteristics of a red-emitting QD-LED. The device was biased at 13 V in vacuum (5×10^{-3} torr) at room temperature.

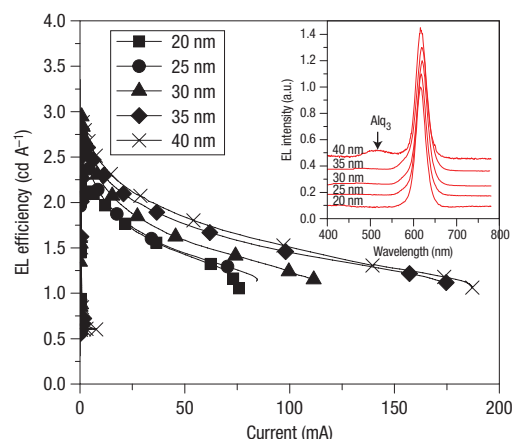


Figure 5 EL efficiency versus current plots of the red-emitting QD-LEDs with an HTL of 45 nm, a QD layer of 2 ML and different ETL thicknesses. The inset shows the EL spectra of QD-LEDs with different ETL thicknesses measured at $\sim 3,000$ cd m^{-2} .

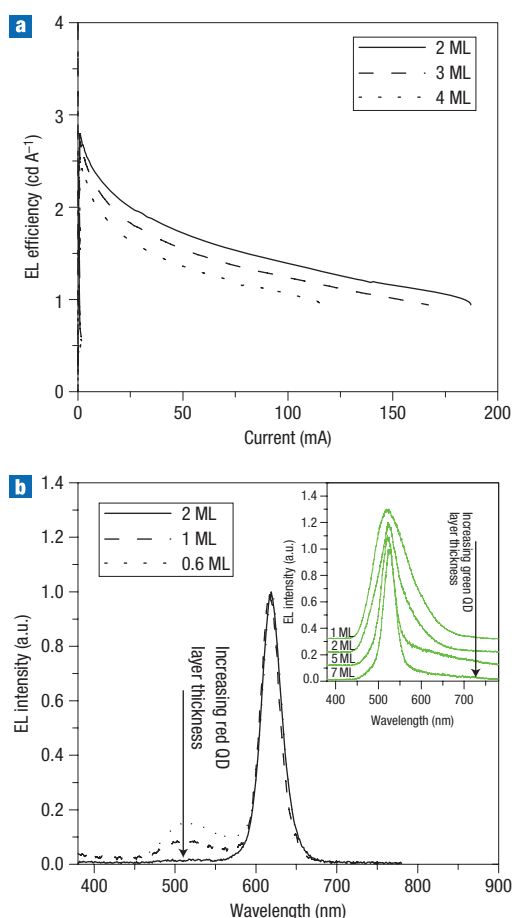


Figure 4 Effect of QD layer thickness on EL performance of the QD-LEDs. **a**, EL efficiency versus current plots for the red-emitting QD-LEDs with different QD layer thicknesses. **b**, EL spectra of the red-emitting QD-LEDs with different QD layer thicknesses operated at $\sim 3,000$ cd m^{-2} . The inset shows the EL spectra of the green-emitting QD-LEDs with different QD layer thicknesses operated at $\sim 3,000$ cd m^{-2} .

OPTIMIZATION OF HTL AND ETL THICKNESSES

In the QD-LEDs, the HTL and ETL thicknesses were both optimized to confine the injected electrons and holes to recombine predominantly within the QD layer and provide optimal hole and electron transportation. The HTL thickness was optimized as 45 nm, at which the device achieved a balance between low turn-on voltage and high luminance/efficiency. With an HTL thickness of <40 nm, although there was lower turn-on voltage, the device efficiency was decreased owing to higher current leakage. With an HTL thickness of >50 nm, the turn-on voltage of the QD-LEDs was increased, and the maximum luminance/efficiency was decreased because inefficient emission from the poly-TPD was involved in the EL process of the QD-LEDs. The optimization of the ETL thickness is particularly important because Alq_3 intrinsically is an efficient green emitter²⁸. Figure 5 shows the EL efficiency of red-emitting QD-LEDs having different ETL thicknesses and a constant HTL thickness (45 nm) and QD layer (2 MLs). The EL efficiency and the maximum injection current were consistently increased with an increase of the ETL thickness from 20 nm to 40 nm. However, at an ETL thickness of 40 nm, the emission of Alq_3 began to appear in the EL spectrum (the inset of Fig. 5), which caused the colour purity of the QD-LED to deteriorate. Therefore, the optimized ETL thickness in the QD-LEDs was 35 nm for achieving high EL efficiency while guaranteeing high colour purity.

The effort reported here represents a further step towards the application of colloidal QD-LEDs featuring bright and saturated colours, low cost and large area. Our results suggest that high-performance multicoloured QD-LEDs can be achieved by simply tailoring the structure of the QDs and optimizing the thicknesses of the HTL, QD emissive layer and ETL.

METHODS

SYNTHESIS AND PURIFICATION OF QDs

CdO , ZnO , Se and S served as precursors to synthesize the CdSe/ZnS core-shell QDs. No organometallic precursor was involved. The starting CdSe core for all four colours was synthesized using well-established methods with emission wavelengths at about 500, 560, 570 and 580 nm. The shell structure of the green and yellow emitters was composed of ZnS , whereas that of the orange and red emitters was CdS/ZnS . The preparation of the core-shell QDs followed the successive ion layer adsorption and reaction (SILAR) method²³.

See Supplementary Information for an explanation of the preparation and purification procedures.

DEVICE FABRICATION AND CHARACTERIZATION

The QD-LED devices were fabricated as follows. The pre-patterned and polished ITO glass substrates were thoroughly cleaned in various solvents and used as the anode after a UV/ozone treatment. PEDOT:PSS was spun-cast from its aqueous solution (Baytron, AL P4083) onto the ITO surface and then subjected to thermal annealing at 150 °C for 15 min. A poly-TPD (ADS 254BE) layer, as an HTL, was prepared by spin-coating its chlorobenzene solution on top of the PEDOT:PSS layer, followed by an annealing treatment at 110 °C for 1 h. The QDs were dissolved in toluene and subjected to a centrifugal treatment to remove the residue. Emissive layers were then prepared by spin-coating the toluene solutions of QDs with controlled concentrations on top of the HTL at 1,000 r.p.m., followed by an annealing treatment at 80 °C for ~30 min. The Alq₃ layer, as an ETL, was prepared by thermal evaporation at a rate of 0.1 nm s⁻¹ on top of the QD layer. Before the thermal evaporation, Alq₃ was subjected to a sublimation treatment. The cathode, Ca over-coated with Al, was thermally deposited through a shade mask at a pressure of <1 × 10⁻⁶ torr. The defined active area of the devices was 4 mm² unless otherwise stated. All processes after the preparation of the PEDOT:PSS buffer layer were performed in a nitrogen-filled glove box. All layer thicknesses were monitored by Ambios XP-2 thickness profiler.

EL spectra were recorded with a Hitachi F-4500 fluorescence spectrophotometer. The current/voltage (*I*–*V*) and luminance/voltage (*L*–*V*) characteristics were measured on a computer-controlled Keithley 236 Source-Measure Unit and a Keithley 2000 Multimeter coupled with a Si photomultiplier tube, which was calibrated by a Photo Research PR650 camera. All the above measurements were performed under ambient conditions. The lifetimes of the QD-LEDs were tested in a vacuum (5 × 10⁻³ torr) at room temperature. An HP 1310 power supply was used to provide the voltage bias, and an unbiased Thorlab TA100 silicon detector of known aperture size was used to read the LED output intensity, which was then converted to luminance. A National Instruments (NI) data logger was used to record the data and, using an analog-to-digital interface, connected with the computer for *in situ* plotting.

DETERMINATION OF THE QD LAYER THICKNESS

The thickness of the QD layer, *t*_{QD}, was determined by measuring the peak absorbance of the QD layer at the first exciton peak position, *A*_{exciton}, and comparing it with the extinction coefficient of QDs, *ε*_{exciton}, according to Lambert–Beer's law:

$$t_{\text{QD}} = \frac{A_{\text{exciton}}}{\varepsilon_{\text{exciton}} C}, \quad (1)$$

where *C* is the molar density (mol L⁻¹) of the QD layer. Determination of the size-dependent *ε*_{exciton} values of CdSe QDs has been discussed²⁹. The extinction coefficient, with the unit of per mol of particles, is related to the particle diameter, *D*, and excitonic transition energy, *ΔE*, by the following equation:

$$\varepsilon_{\text{exciton}} = 1,600\Delta E(D)^3. \quad (2)$$

For the first order of approximation, equation (2) was used to calculate the *ε*_{exciton} of the CdSe/(Zn,Cd)S core-shell structures by replacing the actual particle diameter with an effective value of the plain core structure possessing the same first exciton absorption peak. After obtaining *ε*_{exciton}, the thickness of the QD layers was calculated according to equation (1) and it was expressed as the number of monolayers (MLs) of the QDs.

Received 3 July 2007; accepted 15 October 2007;
published 18 November 2007.

References

- Colvin, V. L., Schlamp, M. C. & Alivisatos, A. P. Light-emitting diodes made from cadmium selenide nanocrystals and a semiconducting polymer. *Nature* **370**, 354–357 (1994).
- Dabbousi, B. O., Bawendi, M. G., Onitsuka, O. & Rubner, M. F. Electroluminescence from CdSe quantum-dot/polymer composites. *Appl. Phys. Lett.* **66**, 1316–1318 (1995).
- Coe, S., Woo, W.-K., Bawendi, M. & Bulović, V. Electroluminescence from single monolayers of nanocrystals in molecular organic devices. *Nature* **420**, 800–803 (2002).
- Zhao, J. *et al.* Efficient CdSe/CdS quantum dot light-emitting diodes using a thermally polymerized hole transport layer. *Nano Lett.* **6**, 463–467 (2006).
- Hikmet, R. A. M., Chin, P. T. K., Talapin, D. V. & Weller, H. Polarized-light-emitting quantum-rod diodes. *Adv. Mater.* **17**, 1436–1439 (2005).
- Coe-Sullivan, S., Steckel, J. S., Woo, W.-K., Bawendi, M. G. & Bulović, V. Large-area ordered quantum-dot monolayers via phase separation during spin-casting. *Adv. Funct. Mater.* **15**, 1117–1124 (2005).
- Schlamp, M. C., Peng, X. & Alivisatos, A. P. Improved efficiencies in light emitting diodes made with CdSe(CdS) core/shell type nanocrystals and a semiconducting polymer. *J. Appl. Phys.* **82**, 5837–5842 (1997).
- Steckel, J. S. *et al.* Color-saturated green-emitting QD-LEDs. *Angew. Chem. Int. Edn* **45**, 5796–5799 (2006).
- Steckel, J. S. *et al.* Blue luminescence from (CdS)ZnS core-shell nanocrystals. *Angew. Chem. Int. Edn* **43**, 2154–2158 (2004).
- Mueller, A. H. *et al.* Multicolor light-emitting diodes based on semiconductor nanocrystals encapsulated in GaN charge injection layers. *Nano Lett.* **5**, 1039–1044 (2005).
- Zhao, J. *et al.* Electroluminescence from isolated CdSe/ZnS quantum dots in multilayered light-emitting diodes. *J. Appl. Phys.* **96**, 3206–3210 (2004).
- Chaudhary, S., Ozkan, M. & Chan, W. C. W. Trilayer hybrid polymer-quantum dot light-emitting diodes. *Appl. Phys. Lett.* **84**, 2925–2927 (2004).
- Gao, M. *et al.* Electroluminescence of different colors from polycation/CdTe nanocrystal self-assembled films. *J. Appl. Phys.* **87**, 2297–2302 (2000).
- O'Connor, E. *et al.* Near-infrared electroluminescent devices based on colloidal HgTe quantum dot arrays. *Appl. Phys. Lett.* **86**, 201114 (2005).
- Steckel, J. S. & Bawendi, M. G. 1.3–1.55 μm tunable electroluminescence from PbSe quantum dots embedded within an organic device. *Adv. Mater.* **15**, 1682–1686 (2003).
- Bakueva, L. *et al.* Size-tunable infrared (1000–1600 nm) electroluminescence from PbS quantum-dot nanocrystals in a semiconducting polymer. *Appl. Phys. Lett.* **82**, 2895–2897 (2003).
- Murray, C. B. & Bawendi, M. G. Synthesis and characterization of monodisperse nanocrystals and close-packed nanocrystal assemblies. *Annu. Rev. Mater. Sci.* **30**, 545–610 (2000).
- Qu, L. & Peng, X. Control of photoluminescence properties of CdSe nanocrystals. *J. Am. Chem. Soc.* **124**, 2049–2056 (2002).
- Coe-Sullivan, S., Steckel, J. S., Kim, L. A., Bawendi, M. G. & Bulović, V. Method for fabrication of saturated RGB quantum dot light emitting devices. *Proc. SPIE* **5739**, 108–115 (2005).
- Li, Y. Q. *et al.* White organic light-emitting devices with CdSe/ZnS quantum dots as a red emitter. *J. Appl. Phys.* **97**, 113501 (2005).
- Xu, J. *et al.* Microcavity light emitting devices based on colloidal semiconductor nanocrystal quantum dots. *IEEE Photon. Technol. Lett.* **17**, 2008–2010 (2005).
- Peng, Z. A. & Peng, X. G. Formation of high-quality CdTe, CdSe, and CdS nanocrystals using CdO as precursor. *J. Am. Chem. Soc.* **123**, 183–184 (2001).
- Li, J. J. *et al.* Large-scale synthesis of nearly monodisperse CdSe/CdS core/shell nanocrystals using air-stable reagents via successive ion layer adsorption and reaction. *J. Am. Chem. Soc.* **125**, 12567–12575 (2003).
- Qu, L., Peng, Z. A. & Peng, X. Alternative routes towards high quality CdSe nanocrystals. *Nano Lett.* **1**, 333–337 (2001).
- Carter, J. C. *et al.* Operating stability of light-emitting polymer diodes based on poly(*p*-phenylene vinylene). *Appl. Phys. Lett.* **71**, 34–36 (1997).
- Sun, Q. J. *et al.* White light from polymer light-emitting diodes: utilization of fluorenone defects and exciplex. *Appl. Phys. Lett.* **88**, 163510 (2006).
- Sun, Q. J., Hou, J. H., Yang, C. H., Li, Y. F. & Yang, Y. Enhanced performance of white polymer light-emitting diodes using polymer blends as hole-transporting layers. *Appl. Phys. Lett.* **89**, 153501 (2006).
- Tang, C. W. & Van Slyke, S. A. Organic electroluminescent diodes. *Appl. Phys. Lett.* **51**, 913–915 (1987).
- Yu, W. W., Qu, L., Guo, W. & Peng, X. Experimental determination of the extinction coefficient of CdTe, CdSe, and CdS nanocrystals. *Chem. Mater.* **15**, 2854–2860 (2003).

Acknowledgements

This work was supported by the Ministry of Science and Technology of China (973 project, No. 2002CB613404) and NSFC (No. 20421101 and 50633050). Y.A.W. acknowledges funding from the National Science Foundation SBIR program (award number: 0638209). We thank Ghassan Jabbour for the calculation of the CIE of the QD-LED emission. Correspondence and requests for materials should be addressed to Y.E.L. or Y.A.W. Supplementary information accompanies this paper on www.nature.com/naturephotonics.

Author contributions

Q.J.S., C.H.Y. and Y.E.L. designed, fabricated and characterized the devices. Y.A.W., L.S.L. and D.Y.W. designed and synthesized the quantum dots. T.Z. and J.X. measured the device lifetimes and calculated the thicknesses of the QD layers.

Reprints and permission information is available online at <http://npg.nature.com/reprintsandpermissions/>